Wear 362-363 (2016) 33–38

Contents lists available at ScienceDirect

Wear

journal homepage: www.elsevier.com/locate/wear

Wear mechanism and morphologic space in ceramic honing process

R.A. Mezari [a,b,*], R.S.F. Pereira [a], F.J.P. Sousa [c], W.L. Weingaertner [d], M.C. Fredel [a]

[a] Ceramic and Composite Materials Research Laboratories - CERMAT, Universidade Federal de Santa Catarina, Florianópolis/SC, Brazil
[b] SENAI Institute of Technology in Materials, Criciúma/SC, Brazil
[c] FBK – Fertigungstechnik und Betriebsorganisation Kaiserslautern, Technische Universität Kaiserslautern, Germany
[d] Laboratory of Mechanical Precision, Universidade Federal de Santa Catarina, Florianópolis/SC, Brazil

ARTICLE INFO

Article history:
Received 7 March 2015
Received in revised form
27 April 2016
Accepted 6 May 2016
Available online 13 May 2016

Keyword:
Wear
Ceramic
Honing
Tribology
Roughness

ABSTRACT

The aesthetic and mechanical properties of porcelain stoneware tiles have promoted their rise in the ceramic tile market. Great part of the aesthetic success is due to the gloss development, which occurs during the honing process. The present study, therefore, aims to focus on this stage of manufacturing process by clarifying the correlation among abrasive size, glossiness and roughness. A clearer interpretation of these parameters is offered, proposing a correction of the unit of measure which is being used in industry and the most of available literature for defining abrasive particle size. Herein, it is concluded that finer particles are those that most contribute to both surface roughness decrease and glossiness development. Not only is the roughness described as a function of the statistical parameters, namely kurtosis and skewness, but also a corresponding morphological space diagram is presented. This series of analyses results in the identification of changes in asperities' morphology taking place in the case of abrasives within a range of 17 – 23 μm, as a consequence of a transition in wear mechanisms.

1. Introduction

Porcelain stoneware is a product with higher technology degree than other ceramic tiles. However, their finishing process remains based on either the application of employees' expertise or empirical knowledge from other materials, such as ornamental stones and glass [1,2]. Moreover, up to 40% of the total production cost is due to the stage of the surface finishing [3]. High water consumption (20–40 l/m^2), tool wear (0.5 kg/m^2) and thickness losses, which occur through the product's thickness up to 10% [4], are factors leading to this high percentage of cost. There is a lack of scientific studies in this research field, which shows that there is a great opportunity to develop new technical and scientific knowledge providing possibilities to optimize the process.

Previous studies have been conducted in order to overcome the lack of knowledge in the field, thereby contributing to an increase of process efficiency. Sousa [5–7] used mathematical models describing the abrasive path in order to create a software tool, which is able to simulate the kinematics of flat honing with lapping kinematics process. Hutchings [8,9] replicated the process in laboratorial scale and studied the relation among abrasive particle size, surface roughness and glossiness. The results showed a greater glossiness increase for abrasive with particle size smaller than 400 mesh (37 μm); while a substantial reduction of surface roughness occurred for abrasives with larges particle size.

One of the subjects for optimizing and understanding this process is the identification of removal mechanisms during the process. Although ceramics are well-known as fragile materials, they may exhibit plastic or viscous flow [10,11] and crack propagation [12] under machining. These two different behaviors (brittle and plastic) give at least two different material removal micro-mechanisms: microcracking (brittle) and microplowing (plastic). The micro-mechanism prevailing in the process also has a great influence on the glossiness development and roughness of the piece. Sanchez [13] showed that abrasives particles smaller than 600 mesh (23 μm) result in grooves with characteristics of plastic flow.

Moreover, several studies have attempted to map the micro-mechanisms transitions in terms of specific parameters. Hsu [14], for example, studied the influence of lubrication and sliding speed for various materials. Hutchings [15] presented a map illustrating that microplowing is more likely to occur with decreasing abrasive particle size and low normal load. Most of these maps are applicable only to a specific tribological system, which limits its use and interpretations. However, Kato [16,17] and Adachi [18] proposed mappings taking into account dimensionless parameters, which were calculated based on toughness, hardness,

* Corresponding author at: CERMAT/Centro Tecnológico – Universidade Federal de Santa Catarina, Caixa Postal 476 – Campus Universitário – Trindade 88040-900 – Florianópolis/SC – Brazil. Tel.: +55 48 96046075.
E-mail address: ramezari@hotmail.com (R.A. Mezari).

http://dx.doi.org/10.1016/j.wear.2016.05.002
0043-1648/

friction and load. Using their methodology, it is possible to achieve maps predicting the wear behavior of a broad range of advanced ceramics.

The present study aims to address the geometrical changes of porcelain surface characteristics during the honing process (which is widely known as polishing). The goal is to correlate the active removal mechanism and a description of the surface morphology using parameters other than the usual average roughness, i.e. using higher order parameters like skewness and kurtosis. Through statistical analysis, the same collected data used for R_a calculation can be used in order to reach additional roughness parameters. Considering the measured surface heights as random events, a probability distribution curve may be achieved. The calculation of central moments based upon the resulting distribution curve leads to values describing e further characteristics of roughness.

The first central moment is the mean of distribution. It represents the asperities average heights, i.e. e. it is related to the average roughness R_a. The second central moment describes the variance [19].

The third central moment, skewness (R_{sk}), describes the curve asymmetry in terms of frequency of valley and peaks along the surface profile. This parameter presents the relation between the number of events above and below the mean line, or in other words, an indicative of the proportion between the amount of peaks and valleys. Profiles where the amount of peaks and valleys are equivalent result in values of $R_{sk}=0$. Profiles with removed peaks or with valley predominance have negative values for R_{sk}. When valleys are fulfilled, forming the pattern of plateau-peak, then R_{sk} becomes positive [19,20].

The fourth central moment is known as kurtosis (R_{ku}) and it describes how distorted from normal the distribution curve is. When $R_{ku}=3$, the curve assumes a Gaussian shape; if $R_{ku}<3$ it shows a thin form and it is called leptokurtic; whereas $R_{ku}>3$, the distributions is flat and called platykurtic [19].

Physically, R_{ku}, gives guidance about the shape of asperities. Values below three indicate the presence of a few high peaks and deep valleys, higher values ($R_{ku}>3$) indicates many low peaks and shallow valleys [20,21].

These two parameters (R_{sk} and R_{ku}) are so important that, if one draws a 2D diagram containing kurtosis and skewness as axes, the so called morphological space is created (Fig. 1). Since each entire distribution of peaks and valley in a given surface profile is represented by a single point, this diagram is an easy way to visualize the evolution of surface characteristics during a process. With it, is possible to distinguish different types of machining processes, as seen in Fig. 1, and also to identify changes in the removal mechanisms regime [22,23].

In the present paper, data obtained from literature and experiments (reproducing the industrial honing process of porcelain tiles on a laboratory scale) are confronted. Consequently, the relation among process parameters (abrasive size and number of contact between abrasive stone and porcelain), resulting properties (roughness and glossiness) and removal phenomena are clarified.

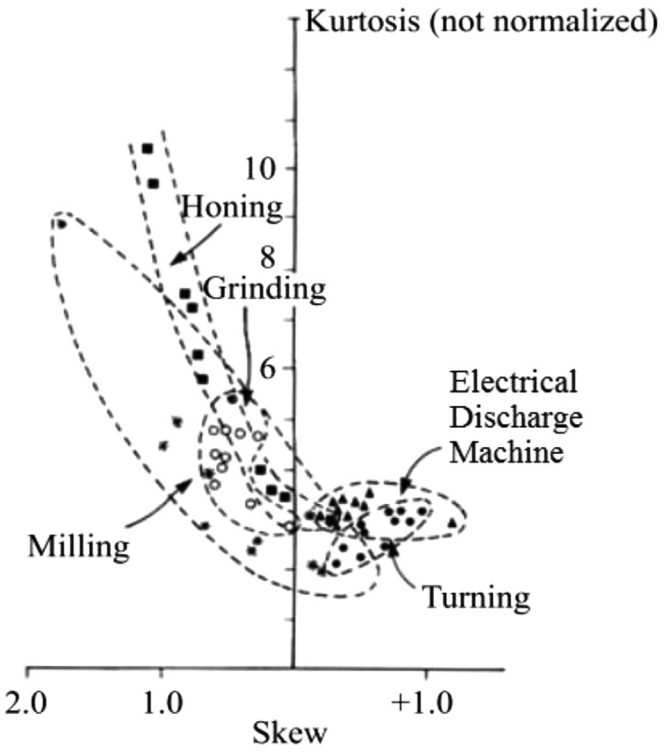

Fig. 1. Typical morphological space for several manufacturing process (adapted from [20]).

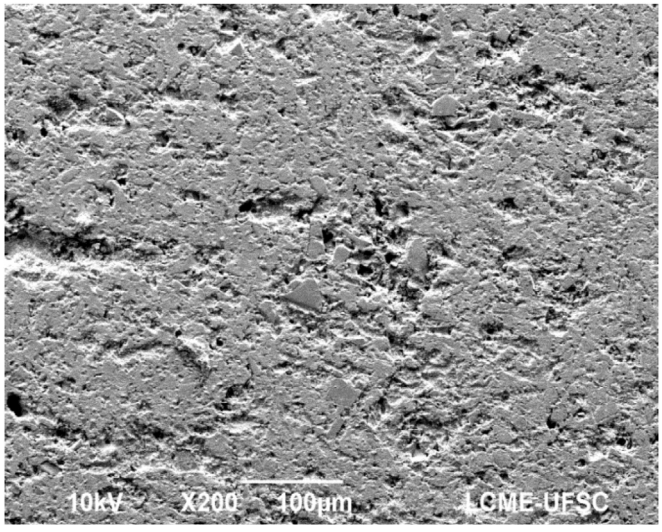

Fig. 2. Porcelain stoneware microstructure.

Table 1
Mechanical properties of porcelain tiles.

Hardness Vickers	Young modulus	Flexural strength	Weibull coefficient
639 HV	72 GPa	61 MPa	7

2. Materials and methods

2.1. Porcelain tiles

The porcelain tiles were acquired as sold, i.e. with their glossiness already developed. Then, the ceramic pieces were reprocessed using the first abrasive stone (36 mesh, 450 μm).

The porcelain microstructure is presented in Fig. 2. The sample was etched in a solution of hydrofluoric acid for 14 min. The image shows a glass matrix with disperse quartz crystals and pores.

Mechanical properties were measured and an overview is presented in Table 1. Hardness measurement was taken on 10 samples (5 points each) with a BUEHLER Vickers microhardness

Table 2
Porcelain composition [wt%].

SiO_2%	Al_2O_3%	Fe_2O_3%	TiO_2%	P_2O_5%	SO_3%	CaO%	MgO%	K_2O%	Na_2O%
69.66	18.94	3.28	0.45	0.029	< 0.065	1.45	0.25	1.86	3.09

Table 3
Characteristics of the honing tool (abrasive stone).

Height	*H*	20 mm
Length	*L*	17.5 mm
Thickness	*e*	14 mm
Curvature radius	*R*	0.133 m
Young Modulus	*E*	21 GPa

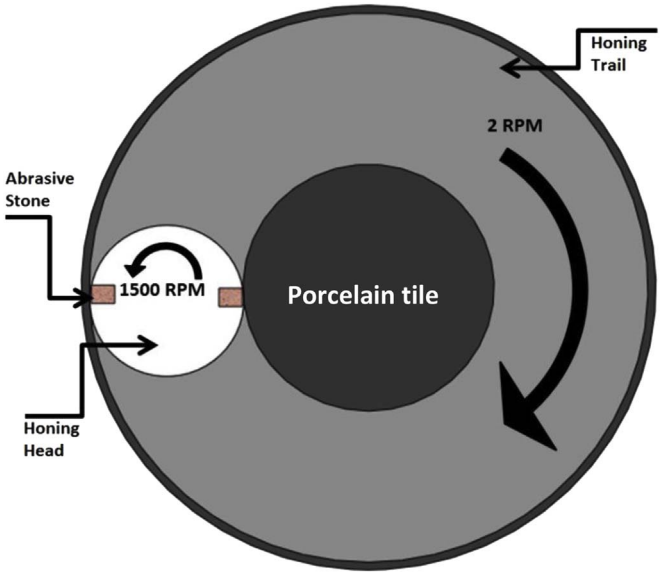

Fig. 3. Honing kinematic used in all experiments.

tester (5 N load). Four points flexural tests were performed in Emic 2000 equipment, and an equipment Sonielastic were used to find the Young modulus.

X-ray fluorescence analyses were used in order to provide the oxides composition of the porcelain tile, which is presented in Table 2.

2.2. Abrasive stones (fickert)

Several blocks of abrasive stone (also known as fickert) were produced by a commercial producer called Fabras Abrasivos, including all grit sizes used at industrial process (36 mesh – 450 μm in the beginning of the process, up to 1500 mesh – 9 μm in the end, giving a total of 17 different particle sizes). The fickerts consist on silicon carbide particles (10%W) embedded in a magnesium oxychloride cement matrix, with additional information shown in Table 3.

2.3. Tribometer

In this work, five porcelain samples for each abrasive sizes were submitted to flat honing with lapping kinematics equipment. This device can perform kinematic settings similar to those used in industries.

The feed speed is reproduced by the rotation of ceramic sample plate. The transverse oscillation motion has been achieved by connecting the honing head (white circle in Fig. 3) to an eccentric axis; however, this movement was deleted from the process in order to obtain a more homogeneous profile of number of contacts between abrasive stone (rectangles in Fig. 3) and porcelain surface. The swinging movement of the abrasive stone (the one which yields a curvature at the contact region) was performed by a device developed by Olenburg [24].

Table 4
Overview of the experimental kinematics setup.

Honing head frequency	f	1500 RPM (25 1/s)
Feed rate	v_{feed}	0.032 m/s
Number of abrasive stones for each test	n_{abr}	2
Outer diameter of honing head	D	115 mm
Inner diameter of honing head	d	80 mm
Cutting speed	V_c	7.65 m/s
Normal load	W	70 N
Linear pressure	P_l	4000 N/m
Contact length	$2b$	0.2 mm
Effective contact pressure	p	12.5 MPa

With this configuration, a circular honing trail was created on the ceramic sample surface (light gray area in Fig. 3). So it was assumed that the tangential velocity at the center of this path is equal to the feed rate v_{feed} (forward speed of tiles inside the Industrial equipment). The tangential velocity was calculated on the middle of the honing trail, for a rotation frequency of porcelain sample of 2 RPM, resulting in $v_{feed}=0.032$ m/s.

The cutting speed V_c was defined as the tangential velocity at the midpoint of the abrasive stone, from where it is estimated that $V_c=7.65$ m/s for a frequency of 1500 RPM. This value lies within the range used by industry [24] which is 5.6 m/s in the inner region of the honing head and up to 12.7 m/s on the peripheral region. An overview of the experimental kinematics setup is shown in Table 4.

To obtain a replicable parameter, the wear duration of the test was replaced by the number of abrasive contact (N_c), i.e. the number of times that a specific point on porcelain tile surface (at the center of honing trail) is touched by any one of the abrasive stones. It may be expressed by Eq. (1), where D is the outer diameter of the honing head and "d" is the distance between the abrasive stones (or the inner diameter of honing head).

$$N_c = \frac{(D-d).n_{abr}.f}{v_{feed}} \quad (1)$$

Ceramic samples with contact numbers N_c between 55 and 1650 were produced for grit sizes from 36 mesh (450 μm) to 800 mesh (17 μm), and between 110 and 3300 N_c for grit sizes 1000, 1200 and 1500 mesh (13 μm, 11 μm, 9 μm, respectively). For each condition (N_c and grit size) five samples were evaluated.

The contact conditions were adjusted to be as similar as possible to those encountered in the industrial facilities, according to Olenburg [24] and Hutchings [3,8]. The normal load $W=70$ N resulted in an effective contact pressure $p=12.5$ MPa, which is within the 10–15 MPa range reported by Hutchings [3,8]. The effective contact pressure is calculated using Hertz equations for elastic contacts, assuming both (tile and abrasive stone) Poisson ratios equal to 0.2 (based on several literatures for similar materials, cements and porcelain such as Watanabe [25], Carter [26] and Odler [27].

2.4. Measurements

After the honing tests, samples were analyzed using an equipment provided by the Laboratory of Optics from University of the State of Santa Catarina – UDESC, a confocal microscope model LEICA 3DCM. All the samples were measured in five positions along the central diameter of the honing trail.

The glossiness was measured by glossimeter model HORIBAIG-320 with five measurements conducted at the central diameter of honing trail, with the data acquired in Gloss Unit (G.U), which is the percentage of reflectance of a surface compared to the equipment standard sample.

3. Results and discussion

3.1. Surface roughness, glossiness and grit size

The chart in Fig. 4 shows the relation among the grit size, surface roughness and glossiness. It shows data of samples with contact number $N_c = 1650$ for grit sizes between 36 mesh (450 μm) and 800 mesh (17 μm), and $N_c = 3300$ contacts for abrasives between 1000 mesh (13 μm) and 1500 mesh (9 μm).

Results show that there is a clear correlation among the decrease of abrasive particle size, the decrease of surface roughness and the glossiness. Initially, with the use of the firsts fickerts (46–400 mesh, 345 – 37 μm), there was a large roughness reduction, which appears to stabilize and slowly decrease for finer abrasives. Glossiness displays a contrary behavior, keeping its value almost stable until the grit size 400 mesh (37 μm). Subsequently glossiness is greatly increased, reaching 69.4 G.U. (gloss units) till 1500 mesh (9 μm).

This information is consistent with the literature [3,8,13]. Based on this data it can be inferred that the coarser abrasives have greater influence on the surface roughness than finest particles, and, that smaller abrasives are the ones responsible for glossiness increase.

However, with this kind of interpretation the relation between roughness and glossiness becomes unclear. As it is seen in Fig. 4, in the region where there is a large reduction in surface roughness (46 mesh to 400 mesh; 345–37 μm), the glossiness remains stable; and in the region where there is great increase in glossiness (600–1500 mesh; 23–9 μm) there is little gain in terms of roughness.

In order to clarify this dependence, it is proposed here to present the data as a function of abrasive particles size or average diameter rather than mesh categories. Fig. 5 shows exactly the same results as Fig. 4, however with the aforementioned change in the abrasive size axis, where an expected average diameter for each particle size was used instead of the grit size (according to Wiggers [28]).

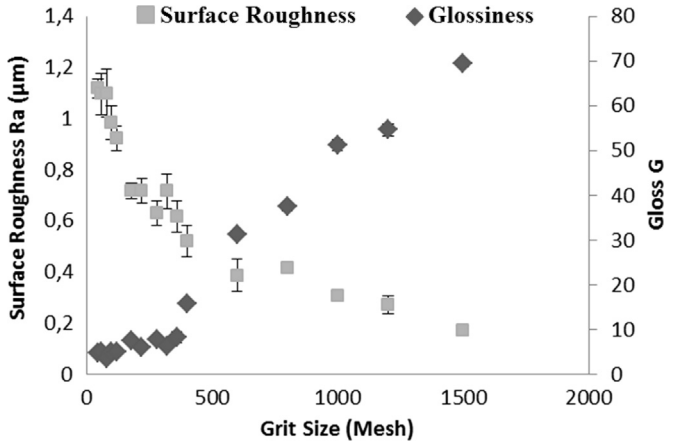

Fig. 4. Influence of decreasing grit size on surface roughness and glossiness.

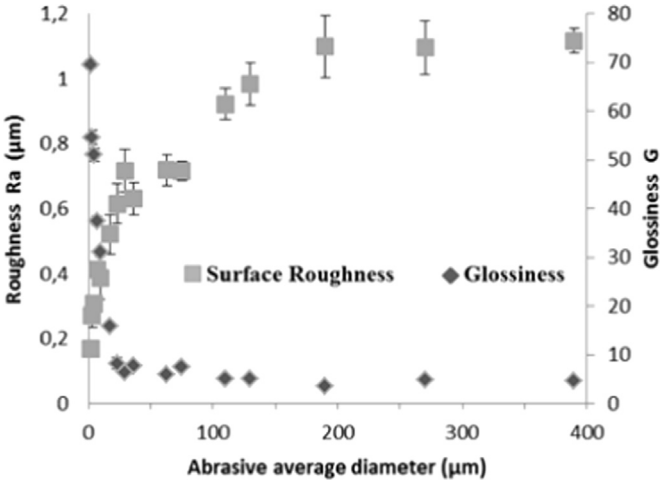

Fig. 5. Influence of abrasive particle size on surface roughness and glossiness.

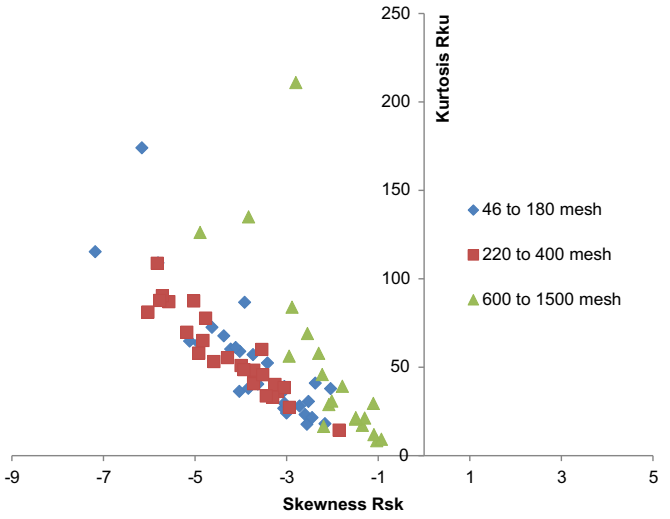

Fig. 6. Morphological space of porcelain flat honing with lapping kinematics. The data is classified in steps according to Bittencourt's classification [29].

The analysis of glossiness and roughness as a function of abrasive diameter (Fig. 5), allows different interpretations from those commonly encountered in the literature for porcelain tile "polishing". First, the glossiness is still more affected by smaller particles (< 50 μm). However, other than before, it is observed that the greater variation in surface roughness also occurs with the use of finest abrasive diameter, and particles larger than 200 μm hardly affect the roughness.

This behavior is consistent with the active removal mechanism (microcraking), since larger particle sizes tend to cause a brittle removal during the ceramic tile honing process [13]. Due to material heterogeneity (hard crystals and defects such as pores), crack propagation may assume random characteristics, then cracks generated by 200 μm abrasive could propagate as far as cracks initiated by 300 μm abrasive, depending on the existence of near defects, consequently resulting in similar surface roughness values.

This kind of approach results in a clearer relationship of glossiness and roughness, since it is shown that the main variation of both parameter occurs for abrasive smaller than 23 μm (600 mesh). This behavior may be correlated to a greater participation of microplowing mechanisms with the use of finer abrasives. No

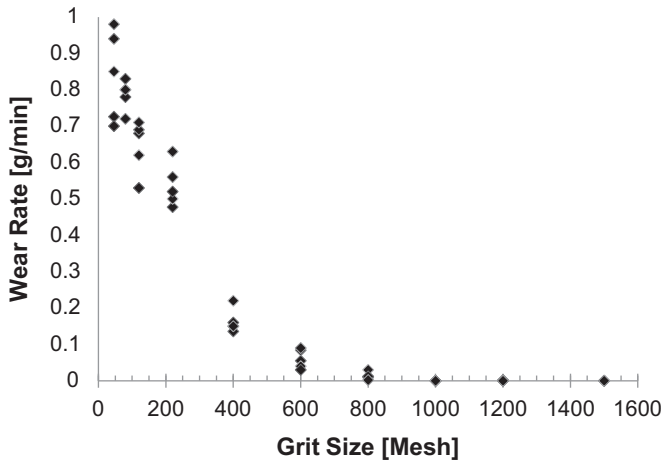

Fig. 7. Wear rate test showing that the material removal ceases for abrasives smaller than 800 mesh (17 μm).

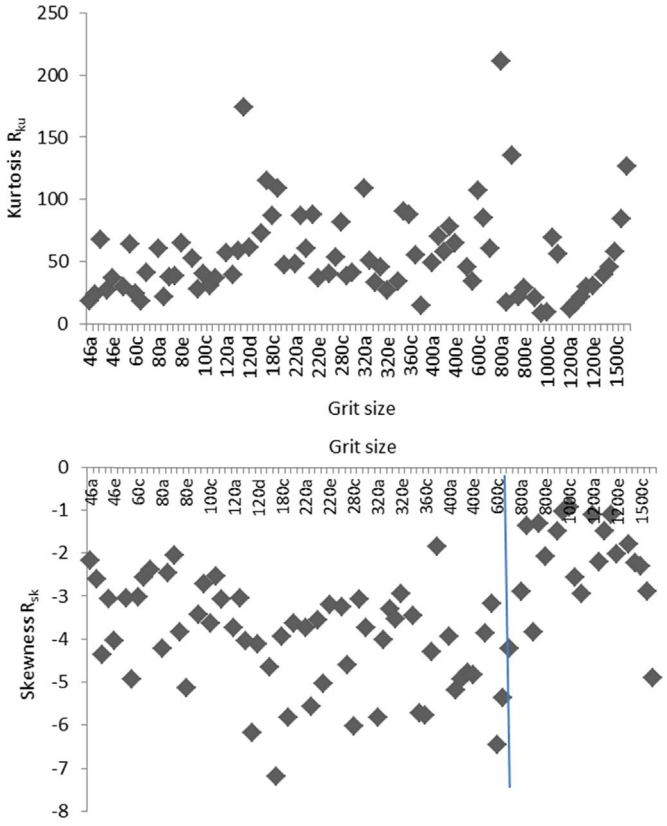

Fig. 8. Variation of the parameters R_{ku} and R_{sk} due to the reduction of grit size.

nucleation and propagation of cracks occurs, so the groove tends to be proportional to the abrasive size, resulting in greater reduction of roughness.

3.2. Morphological space

The first aspect one may notice in the graph of Kurtosis R_{ku} as a function of Skewness R_{sk} (Fig. 6) is that all the measured points are located in the negative quadrant of skewness. This means that the surface roughness profile is characterized by the predominance of valleys over peaks, which as stated by Whitehouse [21], is expected for processes such as honing, polishing and grinding, due to the preferential removal of peaks.

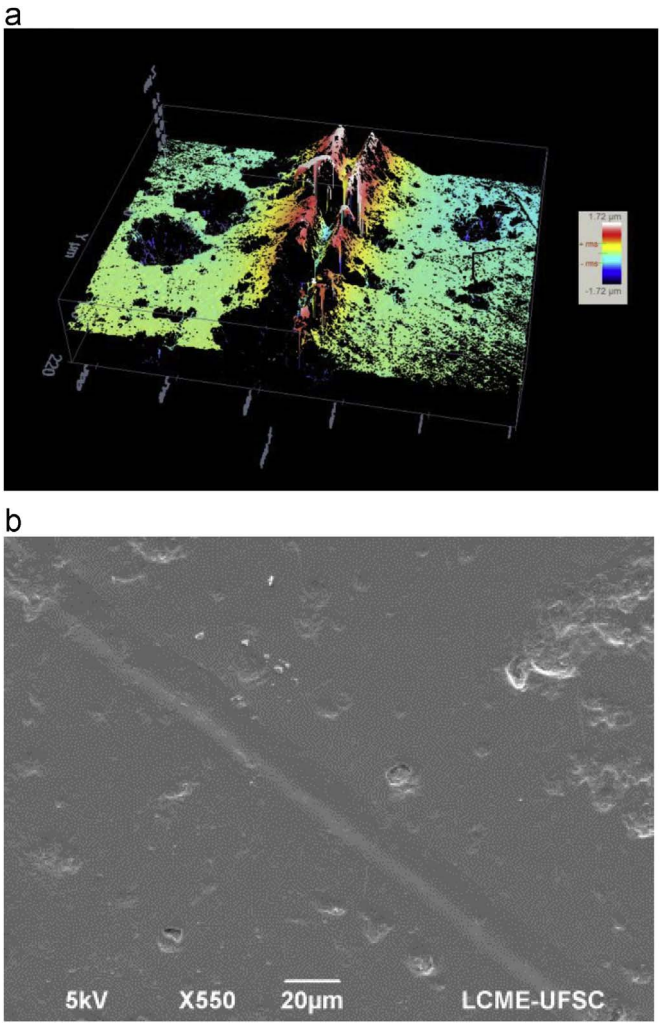

Fig. 9. Confocal microscopy (a) and SEM (b) of a porcelain tile after scratch test with Vickers indenter; 50 mm/s; 1 N.

If the data are classified as proposed by Bittencourt [29], who divided the process in 3 steps according to the abrasive size and effect on the surface, it is noticed that the first two steps produce surfaces whose morphological spaces cannot be distinguished from each other. However, the third step (responsible for the main gain of glossiness) occupies a different position, closer to the axis of $R_{sk}= 0$.

De Mello [22,23] states that this type of arrangement indicates changes in the removal mechanism, and according to Sanchez [13], it makes perfect sense, considering that for abrasives finer than 600 mesh (23 μm) the microplowing mechanism prevails. Also Sousa [30] stated that ductile mechanisms are necessary for high gains in glossiness.

The porcelain wear rate was also measured (Fig. 7) to highlight the change in wear micro-mechanism. It indicated that for 800 mesh (17 μm) abrasive and beyond, no material removal occurs, i. e. the results point out that there is a great modification of surface roughness (as seen in Fig. 5) without mass loss. The reason for this behavior may be explained by the decrease of contact pressure of each abrasive particle, which is a result of the increased number of particles at the abrasive stone that are sharing the load [13]. Besides, as aforementioned, transition from microcracking to microploughing is more likely to occur with low normal load [15].

An isolated analysis of skewness and kurtosis (Fig. 8) shows that after the use of particle size 600 mesh (23 μm) there is a tendency of R_{sk} values to remain concentrated closer to zero, while

R_{ku} has shown high dispersion throughout the process. The letters on the abrasive size axis refers to the number of the experiment.

This curve displacement for values of R_{sk} closer to zero indicates that after the fickert 600 mesh (23 μm), the amount of peaks and valley becomes more balanced. It happens due to material plastic (or viscous) flow, which is displaced and ends up filling the valleys as established by Sousa [30].

Another explanation is the plastic displacement of material to the sides of the groove, as explained by Zum Gahr [31], creating lateral peaks for each groove formed and decreasing the predominance of valleys. This plastic displacement of material to the groove's lateral became evident with the analysis of surface topography performed with confocal microscope on the surface of a porcelain tile subjected to scratch test (Fig. 9).

4. Conclusions

The relationships among abrasive size, wear mechanisms, glossiness and surface roughness of honed tiles were experimentally investigated and quantified. A further analysis of roughness parameter (R_a, R_{sk}, R_{ku}) allowed the following major conclusions about surface characteristics and removal mechanisms:

1) The use of average diameter, instead mesh, as unit for the abrasive particles size classification, has led to a more coherent interpretation of relationship among granulometry, roughness R_a and glossiness.
2) The behavior mentioned before occurred mainly due to a change of removal mechanism that happens between 600 mesh and 800 mesh, or smaller than 23 μm, where finer abrasives are responsible for great modification of surface roughness and glossiness, while no loss of mass is observed.
3) Investigation of roughness parameters such as skewness R_{sk} and kurtosis R_k proved to be useful in order to provide more information about the asperities profile, like the predominance of valleys compared to presence of peaks of the process of porcelain tile finishing.
4) Through the construction of morphological space it was possible to identify the transition of wear/removal mechanisms during the process, which occurred after the use of grit size 600 mesh (23 μm). This identification was possible due to the difference in asperities morphology caused by microploughing and microcracking. Microploughing induces equilibrium between valleys and peaks probably because the flow of material may cover the valleys or generate peaks at the grooves adjacencies. Thus, the investigation of skewness and kurtosis parameters allowed an approach of surface characteristics and removal mechanisms in a single study, clarifying the relation between them.

Acknowledgments

The work was supported by the Deutschland Forschungsgemeinschaft (DFG) and the Coordination for the Improvement of High Education Personnel (CAPES) in the scope of the Brazilian – German Collaborative Research Initiative on Manufacturing Technology. Samples were provided by Cecrisa Revestimentos Cerâmicos S/A and Fabras Química do Brasil.

References

[1] M.J. Ibañes, E. Sáchez, J. García-Ten, M.J. Orts, V. Cantevella, J. Sáchez., C. Soler, J. Portolés, J. Sales, Use of a pin-on-disk tribometer for studying porcelain tile polishing, VII Qualicer, Anais, ITC (2002) 401–416.
[2] A. Tucci, L. Espósito, Polishing of porcelain stoneware tile: surface aspects, VI Qualicer (2000) 127–136.
[3] I.M. Hutchings, K. Adachi, E. Sánchez, M.J. Ibañes, M.F. Quereda, Analysis and laboratory simulation of an industrial polishing process for porcelain ceramic tiles, J. Eur. Ceram. Soc. 25 (13) (2005) 3151–3156.
[4] M.J. Ortiz, E. Sánchez, J. García-Ten, M.J. Ibañes, J. Sanchez., C. Soler, J. Portoles, Comportamiento del gres porcelánico durante la operación de pulido, Bol. Soc. Española Céram. Vidrio 40 (6) (2001) 447–455.
[5] F.J.P. Sousa, J.C. Aurich, W.L. Weingaertner, O.E. Alarcon, Kinematics of a single abrasive particle during the industrial polishing process of porcelain stoneware tiles, J. Eur. Ceram. Soc. 27 (10) (2007) 3183–3190.
[6] F.J.P. Sousa, W.L. Weingaertner, O.E. Alarcon, Computational simulation of the polishing process of porcelain stoneware tiles, Qualicer X (2008) 359–367.
[7] F.J.P. Sousa, J.C. Aurich, W.L. Weingaertner, O.E. Alarcon, Optimization of the kinematics available in the polishing process of ceramic tiles by computational simulations, J. Am. Ceram. Soc. 92 (1) (2009) 41–48.
[8] I.M. Hutchings, Y. Xu., E. Sánchez, M.J. Ibáñes, M.J. Orts, V. Cantavella, Development of surface finish during the polishing of porcelain ceramic tiles, J. Mater. Sci. 40 (2005) 37–42.
[9] I.M. Hutchings, Y. Xu, E. Sánchez, M.J. Ibáñes, M.F. Quereda, Porcelain tile microstructure: implications for polishability, J. Eur. Ceram. Soc. 26 (6) (2006) 1035–1042.
[10] C.J. Evans, E. Paul, D. Dornfeld, D.A. Lucca, G. Byrne, M. Tricard, F. Klocke, Material removal mechanisms in lapping and polishing, CIRP Ann – Manuf. Process 52 (2) (2003) 611–633.
[11] R. Komanduri, On material removal mechanisms in finishing of advanced ceramics and glasses, CIRP Ann. 45 (1996) 509–514.
[12] J.B. Watchman, W.R. Cannon, M.J. Matthewson, Mechanical Properties of Ceramics, John Wiley & Sons (2009), p. 550.
[13] E. Sanchéz, J. Garcia-Ten, M.J. Ibáñes, M.J. Orts, V. Cantavella, Polishing porcelain tile. Part 1: wear mechanism, Am. Ceram. Soc. Bull. 81 (2002) 50–54.
[14] S.M. Hsu, M.C. Shen, Ceramic wear map, Wear 200 (1–2) (1996) 154–175.
[15] I.M. Tribology Hutchings, Friction and Wear of Engineering Materials, Elsevier Science, Oxford (1992), p. 272.
[16] K. Kato, Micro-mechanisms of wear – wear modes, Wear 153 (1992) 277–295.
[17] K. Kato, K. Adachi, Wear of advanced ceramics, Wear 253 (2002) 1097–1104.
[18] K. Adachi, K. Kato, N. Chen, Wear map of ceramics, Wear 203–204 (1997) 291–301.
[19] E.S. Gadelmawla, M.M. Koura, T.M.A. Maksoud, I.M. Elewa, H.H. Soliman, Roughness parameters, J. Mater. Process. Technol. 123 (2002) 133–145.
[20] B. Bhushan, Modern Tribology Handbook, vol. 1, CRC Press (2000), p. 1760.
[21] D.J. Whitehouse, Handbook of Surface and Nanometrology, 2nd ed, CRC Press (2011), p. 978.
[22] D.E. Mello, J.D.B. Durand-Charre, M. Abrasion, Mechanisms of white cast iron I: influence of the metallurgical structure of molybdenum white cast irons, Mater. Sci. Eng. 73 (1985) 203–213.
[23] D.E. Mello, J.D.B. Durand-Charre, M. Abrasion, Mechanisms of white cast iron II: influence of the metallurgical structure of V–Cr white cast irons, Mater. Sci. Eng. 78 (1986) 127–134.
[24] A. Olenburg, F.J.P. Sousa, J.C. Aurich, Polishing of porcelain tiles in industrial – and laboratory-scale, CFI – Ceram. Forum Int. 90 (3) (2013) E39–E43.
[25] T. Watanabe, Analytical research on method for applying interfacial fracture mechanics to evaluate strength of cementitious adhesive interfaces for thin structural finish details. Nanocomposites with unique properties and applications, in: John Cuppoletti (Ed.), Medicine and Industry, InTech, 2011, ISBN: 978-953-307-351-4, doi: 10.5772/18916.
[26] C.B. Carter, M.G. Norton, Ceramic Materials: Science and Engineering, 2nd Ed, Springer, New York (2013), p. 766.
[27] I. Odler, Special Inorganic Cements, CRC Press (2000), p. 416.
[28] W.S. Wiggers, R.A. Santos, D. Hotza, Evolução da superfície do porcelanato ao longo do processo de polimento, Cerâm. Ind. 6 (½) (2007).
[29] E.L. Bittencourt, E. Benincá, Aspectos superficiais do produto grês polido, Cerâm. Ind. 7 (4) (2002) 40–46.
[30] F.J.P. Sousa, Polishing, CIRP, International Academy for production Engineering Research (Ed.), Encyclopedia of Production Engineering, 2014, pp. 957–962, doi: 10.1007/978-3-642-20617-7_6434.
[31] Z.U.M. Gahr, Karl-Heinz, Microstructure and Wear of Materials, Elsevier Science Publishing Company, New York (1987), p. 560.